INSTITUTE OF PHYSICS PUBLISHING JOURNAL OF PHYSICS G: NUCLEAR AND PARTICLE PHYSICS

J. Phys. G: Nucl. Part. Phys. **28** (2002) 1721–1728 PII: S0954-3899(02)33049-4

Centrality dependence of K^0_s, Λ and $\bar{\Lambda}$ production in Au+Au collisions at $\sqrt{s_{NN}}$ = 130 GeV

Matthew A C Lamont for the STAR Collaboration[1]

The University of Birmingham, Birmingham, UK

E-mail: m.a.c.lamont@bham.ac.uk

Received 25 January 2002
Published 10 June 2002
Online at stacks.iop.org/JPhysG/28/1721

Abstract

We report preliminary results on the centrality dependence of both Λ and $\bar{\Lambda}$ production as a function of centrality at mid-rapidity in Au+Au collisions at $\sqrt{s_{NN}} = 130$ GeV in the STAR detector. Data are measured in five different centrality classes which cover the most central 75% of the cross-section. In the case of Λ and $\bar{\Lambda}$, the transverse mass spectra are best described by a Boltzmann function with inverse slope parameters which vary from ∼320 MeV in the most central collisions to ∼260 MeV in the non-central collisions. The K^0_s, however, are best described by a simple exponential fit though their inverse slopes show the same behaviour, decreasing from ∼290 MeV to ∼270 MeV. It is also found that the yields of the K^0_s, Λ and $\bar{\Lambda}$ increase linearly with increasing multiplicity in the collision, while the $\bar{\Lambda}/\Lambda$ shows no significant centrality dependence.

1. Introduction

The ultimate goal of ultra-relativistic heavy-ion collisions is to create a deconfined state of matter, governed by quark and gluonic degrees of freedom, often referred to as the quark–gluon plasma (QGP) [1]. It has long been predicted that an enhancement of strange hadrons is a signature that this deconfined phase occurs during the evolution of relativistic heavy-ion collisions [2]. In order to calculate an enhancement, it is necessary to compare data with a system where deconfinement is not expected to occur. In the absence of p+p, p+A and even light A+A collisions at $\sqrt{s_{NN}} = 130$ GeV, it is informative to compare central Au+Au with peripheral Au+Au collisions. This paper will present results on $\bar{\Lambda}/\Lambda$ ratios as a function of centrality as well as K^0_s, Λ and $\bar{\Lambda}$ yields at mid-rapidity ($|y| < 0.5$), obtained using the STAR detector which is described in detail in [3] and [4].

[1] For a complete list of the STAR Collaboration, see [3].

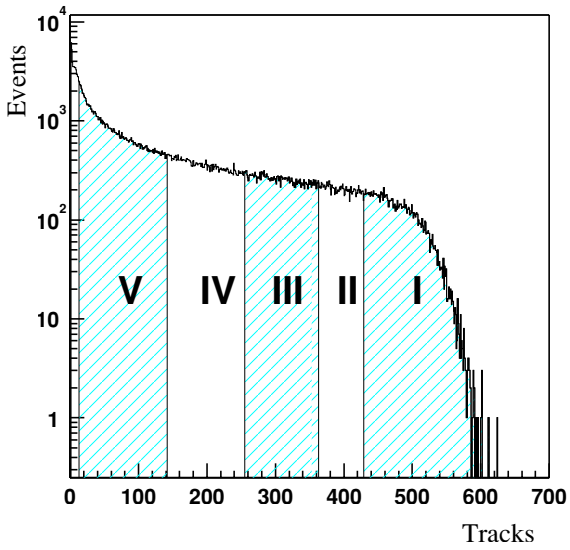

Figure 1. The raw track distribution in the TPC in the range $|\eta| \leqslant 0.5$, showing the five selected centrality bins.

Table 1. The centrality bins used in this analysis, their definition in terms of the cross-section and the raw yields per centrality bin, where bin I represents the 5% most central collisions.

Centrality bin	Cross-section	Λ yield	$\bar{\Lambda}$ yield	K^0_s yield
I	0% $\rightarrow$ 5%	5688	4041	9392
II	5% $\rightarrow$ 10%	4547	3357	8518
III	10% $\rightarrow$ 20%	7488	5412	14398
IV	20% $\rightarrow$ 35%	7502	5488	15053
V	35% $\rightarrow$ 75%	5717	4453	12723

2. Dataset

In order to calculate the centrality of the collision, cuts are placed on the raw TPC track distribution in the range $|\eta| \leqslant 0.5$, as shown in figure 1, obtained using a minimum bias trigger [3]. The values of the bin edges of the raw track distribution are converted to the corrected negative hadron (h^-) distribution and from this, the value of the total hadronic cross-section is calculated [5].

The values of the cross-section corresponding to each centrality bin are tabulated in table 1, along with the raw yields of the K^0_s, Λ and $\bar{\Lambda}$. The binning was chosen so that the raw yields are approximately constant in each of the five centrality bins. The first two centrality bins overlap with the dataset from the central trigger, which yields an order of magnitude greater raw signal and hence allows the measured p_t range to be increased.

The K^0_s, Λ and $\bar{\Lambda}$ are reconstructed via their weak decays in the TPC ($K^0_s \rightarrow \pi^+\pi^-$, $\Lambda \rightarrow p\pi^-$ and $\bar{\Lambda} \rightarrow \bar{p}\pi^+$). Each negative track in the TPC is paired with each positive track to determine the distance of the closest approach between the tracks. If this is less than 1 cm, the momentum vector of the parent particle is extrapolated back to the measured interaction vertex, to determine the validity of the candidate. After this process a large background remains; therefore, various other geometrical cuts are applied to the candidates in order to separate

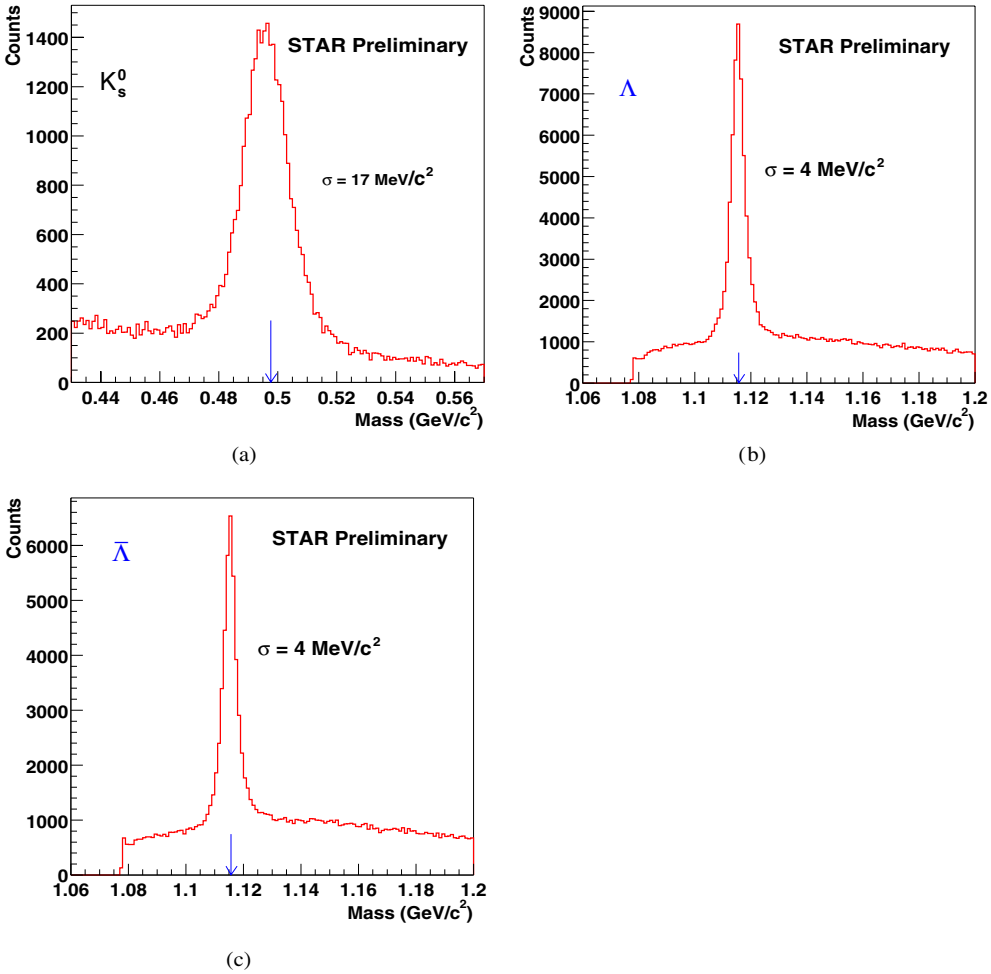

Figure 2. Masses of the K^0_s, Λ and $\bar{\Lambda}$ respectively, for 50 K minimum bias events covering all p_t.

the signal from the largely combinatorial background. A minimum decay length of the V0, and a requirement that the V0 originate from the interaction vertex are two examples of such geometrical cuts. Particle identification cuts, applied to the daughter tracks of the candidates, supplement the geometric cuts and increase the signal-to-background ratio significantly. An example of the mass plots of the K^0_s, Λ and $\bar{\Lambda}$ for 50 000 minimum bias events is given in figure 2, where the mass is determined by assuming the identity of the negative and positive daughters.

The raw yields of the K^0_s are obtained by fitting a Gaussian together with a second-order polynomial background function to the mass histogram, and extracting the area of the Gaussian. As the Gaussian function does not describe the Λ and $\bar{\Lambda}$ distributions very well, Λ and $\bar{\Lambda}$ yields are extracted by simply counting the entries in the invariant mass histograms within a window of 30 MeV/c^2 centred on the expected value [6], as indicated by the arrows in figure 2. The background is then subtracted by summing the entries in two windows on either side of the signal region, each of width 15 MeV/c^2. Only this process can be applied as the background running under the mass peaks is linear in discrete p_t bins. In the case of the K^0_s, this bin-counting method gives comparable results to the fitting method.

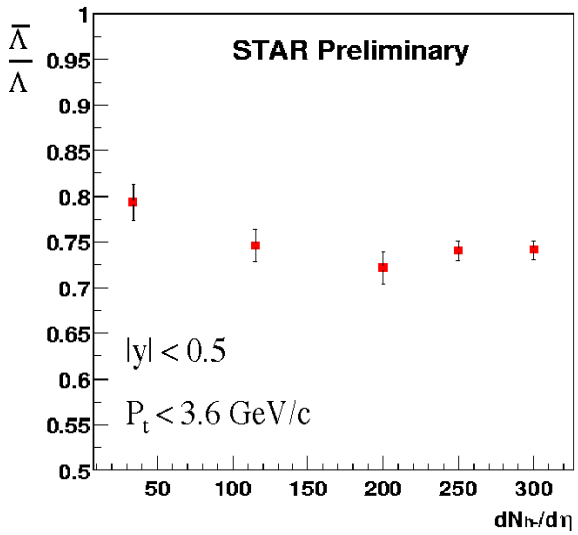

Figure 3. The uncorrected $\bar{\Lambda}/\Lambda$ ratio plotted against the corrected $dN_{h^-}/d\eta$, which is a measure of the centrality of the collision.

3. Ratios

The $\bar{\Lambda}/\Lambda$ ratio can be calculated for each of the five centrality bins. For the most peripheral Au+Au collisions, the ratio should tend to what is observed in p+p data, which could differ from the central heavy-ion collisions depending on the amount of baryon stopping that is present.

Figure 3 shows the ratio for the same five centrality bins plotted versus the corrected value of $dN_{h^-}/d\eta$, and shows a slight rise ($\sim$10%) in the most peripheral bin. More data would be required to investigate this trend further, but it should be noted that the same rise is observed in the $\bar{p}/p$ ratio at the same energy, where more centrality bins are available due to higher statistics [7].

The $\bar{\Lambda}/\Lambda$ ratio was reported to be flat as a function of centrality in Pb+Pb collisions at $\sqrt{s_{NN}} \simeq 17$ GeV at the SPS by WA97, whose four centrality bins covered the most central 40% of the cross-section [10]. However, an increase in the ratio of a factor of 3 was observed by WA97 when comparing p+Be collisions to Pb+Pb.

The ratios have been corrected for the absorption effects of interactions with the detector material, calculated using a GEANT simulation of the detector. The ratios have not been corrected for efficiency or feed-down, but can be used under the assumption that the efficiencies for the Λ and $\bar{\Lambda}$ are equal, as the detector is charge symmetric. Preliminary results using the corrections used to obtain the yields in the next section bear this fact out.

4. Corrected yields

The corrected yields were obtained by generating Monte Carlo (MC) K^0_s, $\bar{\Lambda}$ and Λ particles respectively using a GEANT simulation of the detector set-up [8]. These particles were then mixed into real events, where a detailed TPC response simulation was used to generate information on charge clusters on the TPC pads for the MC tracks. The same event reconstruction was used on these mixed events as on the raw data, while an association

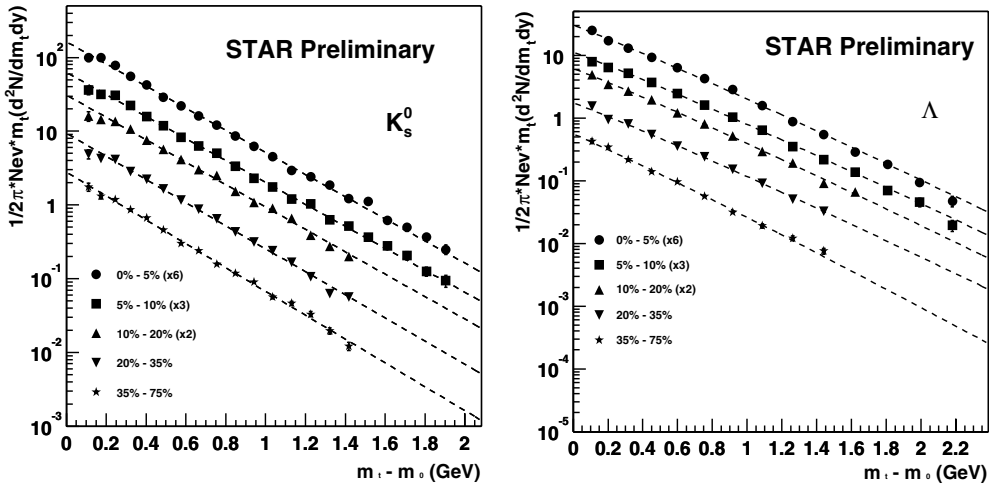

(a) (b)

Figure 4. Transverse mass distributions of the K^0_s and Λ respectively, as a function of collision centrality, where only statistical errors are shown. Most central bins use the central dataset and have been multiplied by a constant factor to aid viewing.

Table 2. Fit parameters from an exponential fit to the K^0_s m_T spectra, and Boltzmann fits to the Λ and $\bar{\Lambda}$ m_T spectra. Both statistical (the first) and systematic errors are presented.

Centrality		0–5%	5–10%	10–20%	20–35%	35–75%
$\frac{dN}{dy}$	K^0_s	$38.9 \pm 0.7 \pm 1.9$	$30.1 \pm 0.6 \pm 1.5$	$21.8 \pm 0.6 \pm 1.1$	$12.6 \pm 0.3 \pm 0.6$	$3.6 \pm 0.1 \pm 0.2$
	Λ	$17.5 \pm 0.4 \pm 1.8$	$13.9 \pm 0.4 \pm 1.4$	$10.9 \pm 0.3 \pm 1.1$	$6.2 \pm 0.2 \pm 0.6$	$1.62 \pm 0.05 \pm 0.2$
	$\bar{\Lambda}$	$12.7 \pm 0.3 \pm 1.3$	$9.9 \pm 0.2 \pm 1.0$	$7.7 \pm 0.2 \pm 0.8$	$4.6 \pm 0.1 \pm 0.5$	$1.29 \pm 0.04 \pm 0.1$
	K^0_s	$289 \pm 3 \pm 17$	$291 \pm 3 \pm 17$	$286 \pm 5 \pm 17$	$278 \pm 4 \pm 17$	$269 \pm 4 \pm 16$
T	Λ	$307 \pm 6 \pm 28$	$308 \pm 6 \pm 28$	$299 \pm 6 \pm 27$	$290 \pm 6 \pm 26$	$260 \pm 5 \pm 24$
(MeV)	$\bar{\Lambda}$	$318 \pm 6 \pm 30$	$307 \pm 6 \pm 30$	$309 \pm 6 \pm 30$	$289 \pm 6 \pm 27$	$261 \pm 5 \pm 25$

technique was applied in order to match the MC and reconstructed information of the generated particles. This association information was used to calculate a correction factor as a function of $p_t(m_t)$ which was then applied to the data. The corrected K^0_s m_t distributions for all five centrality bins are shown in figure 4. They are fitted with a simple exponential function (see equation (1)) to extract the inverse slope (T in MeV) and yield (dN/dy).

$$\frac{1}{2\pi m_t}\frac{d^2N}{dm_t dy} = \frac{dN/dy}{2\pi T(m_0+T)} e^{\frac{-(m_t-m_0)}{T}}. \quad (1)$$

The extracted data for the K^0_s are given in table 2.

The same process is applied to Λ and $\bar{\Lambda}$, where the distributions for Λ are also shown in figure 4. In the case of Λ and $\bar{\Lambda}$, the single exponential given in equation (1), no longer gives the best fit to the data; instead, the distributions are best described by a Boltzmann distribution.

$$\frac{1}{2\pi m_t}\frac{d^2N}{dm_t dy} = \frac{m_t dN/dy}{2\pi T\left(m_0^2+2m_0T+2T^2\right)} e^{\frac{-(m_t-m_0)}{T}}. \quad (2)$$

The dN/dy and inverse slope parameters obtained from this fit are also given in table 2. The yields are not corrected for feed-down from weak decays of multiply strange hadrons.

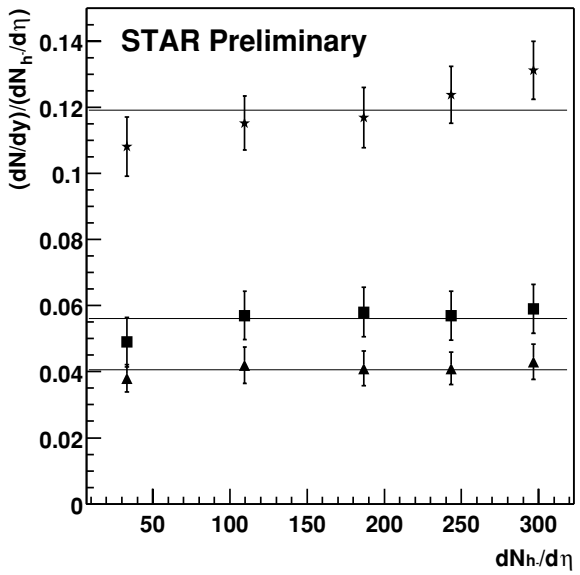

Figure 5. The ratio of the measured $\mathrm{d}N/\mathrm{d}y$ of K^0_s (star), Λ (square) and $\bar{\Lambda}$ (triangle) to the measured $\mathrm{d}N_{\mathrm{h}^-}/\mathrm{d}\eta$ for the five centrality bins. The error bars include the calculated systematic errors.

Table 3. The relationship between the K^0_s, Λ and $\bar{\Lambda}$ yields and the h^- yield, as a function of centrality, presented from this analysis and compared to published data from the SPS [10].

	$\frac{\mathrm{d}N_{y0}/\mathrm{d}y}{\mathrm{d}N_{\mathrm{h}^-}/\mathrm{d}\eta}$	
Particle	This analysis	SPS data
K^0_s	$(0.118 \pm 0.003)\mathrm{h}^-$	$(0.138 \pm 0.013)\mathrm{h}^-$
Λ	$(0.056 \pm 0.003)\mathrm{h}^-$	$(0.086 \pm 0.005)\mathrm{h}^-$
$\bar{\Lambda}$	$(0.042 \pm 0.001)\mathrm{h}^-$	$(0.011 \pm 0.001)\mathrm{h}^-$

Figure 5 represents the ratios of the yields of the K^0_s, Λ and $\bar{\Lambda}$ respectively to the measured h^- yield, which is measured as a function of pseudo-rapidity. In all three cases, the yield increases approximately linearly with the h^- multiplicity. The linear fits to the data, indicated on the figure, give $\mathrm{K}^0_\mathrm{s} = (0.119 \pm 0.004)\mathrm{h}^-$, $\Lambda = (0.056 \pm 0.003)\mathrm{h}^-$ and $\bar{\Lambda} = (0.041 \pm 0.002)\mathrm{h}^-$ respectively, where again, the feed-down correction has not been applied to the Λ and $\bar{\Lambda}$ data. This is indicative of the same production mechanisms of strangeness for all collisions.

The $\mathrm{K}^0_\mathrm{s}/\mathrm{h}^-$ value compares well with what was observed at the CERN SPS (given in table 3), though differences are observed for Λ and $\bar{\Lambda}$. The feed-down contribution to the Λ yield from the Ξ^- and Ξ^0 only, is estimated to be $23.8 \pm 2.0\%$ by using a preliminary measurement of the Ξ^- yield [9] together with information from Ξ^- and Ξ^0 embedding. Therefore, after applying this correction, the Λ/h^- value is approximately half of the SPS value, whilst the $\bar{\Lambda}/\mathrm{h}^-$ is approximately 3 times the SPS value. This behaviour in the Λ/h^- ratio is predicted in thermal models [11], whose applicability to STAR data is discussed further in [12].

Another striking feature of the data in table 2 is the behaviour of the inverse slope with collision centrality. For each centrality bin, the measured slopes of Λ and $\bar{\Lambda}$ are consistent with each other. Also, the inverse slopes for all three particle species decrease with decreasing

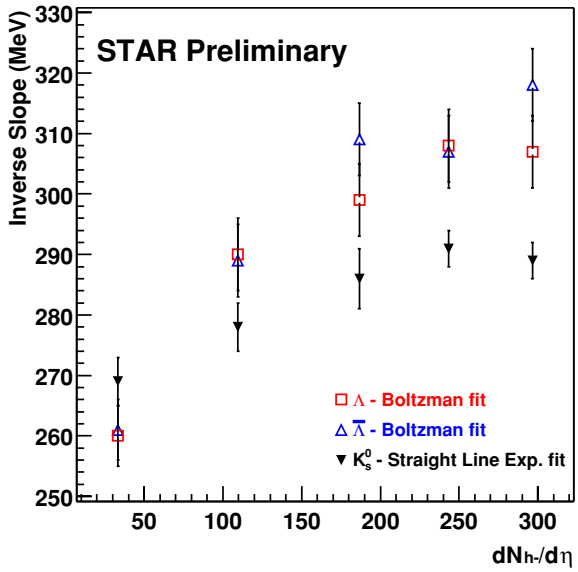

Figure 6. The inverse slopes of the K^0_s (filled triangle), $\bar{\Lambda}$ (open triangle) and Λ (open square) for the five centrality bins. The error bars are statistical only.

collision centrality, with the largest drop in the most peripheral bin, as shown in figure 6. This behaviour, also observed for $\bar{p}$ [13], is indicative of an increase in the collective velocity in the most central collisions, assuming a common freeze-out temperature [14, 15]. Note that while the temperatures appear to be similar, different functions were used to fit the data, and if the same functional form is used, a difference of ∼50 MeV is found between $\Lambda(\bar{\Lambda})$ and K^0_s, as outlined in [9].

5. Conclusions

In this paper we have presented results of the centrality dependence of K^0_s, Λ and $\bar{\Lambda}$ production at mid-rapidity at $\sqrt{s_{NN}} = 130$ GeV in the STAR detector. In all cases, the yields were found to increase linearly with respect to increasing h^- multiplicity. The measured inverse slopes indicate the presence of a strong collective flow, which has a significant dependence on collision centrality. The slopes decrease by between ∼20 MeV and ∼60 MeV when comparing the most peripheral collisions with the most central collisions. The $\bar{\Lambda}/\Lambda$ ratio has also been measured, and is observed to be only loosely dependent on centrality, increasing by ∼10% when going from the most central to the most peripheral collisions.

Acknowledgments

We wish to thank the RHIC Operations Group and the RHIC Computing Facility at Brookhaven National Laboratory, and the National Energy Research Scientific Computing Center at Lawrence Berkeley National Laboratory for their support. This work was supported by the Division of Nuclear Physics and the Division of High Energy Physics of the Office of Science of the US Department of Energy, the United States National Science Foundation,

the Bundesministerium fuer Bildung und Forschung of Germany, the Institut National de la Physique Nucleaire et de la Physique des Particules of France, the United Kingdom Engineering and Physical Sciences Research Council, Fundacao de Amparo a Pesquisa do Estado de Sao Paulo, Brazil, the Russian Ministry of Science and Technology and the Ministry of Education of China and the National Science Foundation of China.

References

[1] For reviews and recent developments see 2002 *Proc. Quark Matter 2001 Nucl. Phys.* A **698** 1c
[2] Müller B and Rafelski J 1982 *Phys. Rev. Lett.* **48** 1066
[3] Barnby L S (STAR Collaboration) 2002 *J. Phys. G: Nucl. Part. Phys.* **28** 1535
[4] Wieman H *et al* (STAR Collaboration) 1997 *IEEE Trans. Nucl. Sci.* **44** 671
[5] Adler C *et al* (STAR Collaboration) 2001 *Phys. Rev. Lett.* **87** 112303
[6] Particle Data Group 1998 *Eur. Phys. J.* C **3** 207
[7] Adler C *et al* (STAR Collaboration) 2001 *Phys. Rev. Lett.* **86** 4478
[8] Brun R *et al* 1987 GEANT user guide *Report DD/EE/*84-1 (CERN)
[9] Castillo J (STAR Collaboration) 2002 *J. Phys. G: Nucl. Part. Phys.* **28** 1987
[10] Antinori F *et al* (WA97 Collaboration) 1999 *Nucl. Phys.* A **661** 130c
[11] Braun-Munzinger P, Magestro D, Redlich K and Stachel J 2001 *Phys. Lett.* B **518** 41
[12] Van Buren G (STAR Collaboration) 2002 *J. Phys. G: Nucl. Part. Phys.* **28** 2103
[13] Adler C *et al* (STAR Collaboration) 2001 *Phys. Rev. Lett.* **87** 262302
[14] Bearden I G *et al* (NA44 Collaboration) 1997 *Phys. Rev. Lett.* **78** 2080
[15] Appelshäuser H *et al* (NA49 Collaboration) 1998 *Eur. Phys. J.* C **2** 661